Supplementary Material

Intra- and Interbrain Synchrony of Guitarist Quartet and Audience during a Concert

Viktor Müller and Ulman Lindenberger

The program of the concert

Piece of music	Composer
Aragonaise	Georges Bizet
Libertango	Astor Piazolla
Merry christmas Mr. Laurence	Ryuichi Sakamoto
Baiao de Gude	Paulo Bellinati
Comme un Tango	Patrick Roux
Dredlocked	Andrew York
Five piezas artesanales	Maximo Diego Pujol
Mediodia en Belgrano	
Alguna calle gris	
Plaza Miserere	
Tangazo a medianoche	
Un domigo en La Boca	
Danza Ritual del Fuego	Manuel De Falla
Säbeltanz (Bonus)	Aram Chatschaturjan

For a better idea of the performance, see Supplementary Video 1.

For dynamic changes of the community structure in real time, see Supplementary Video 2.

The three pieces of music analyzed in the study are available online as audio files (MP3).

The time stamps of SOIs in the three pieces of music (M1, M2, and M3) in the MP3 files:

M1/SOI1: 0:44-1:04; M1/SOI2: 1:05-1:25; M1/SOI3: 1:34-1:54.

M2/SOI1: 0:01-0:21; M2/SOI2: 0:22-0:42; M2/SOI3: 3:40-4:00.

M3/SOI1: 0:02-0:22; M3/SOI2: 0:26-0:46; M3/SOI3: 1:41-2:01.

Network construction and network topology measures

Threshold determination and network costs

In order to remove noisy or spurious connectivity links and emphasize key topological properties of the network, a threshold has to be applied to the connectivity matrix. In general, the choice of a threshold plays an important and non-trivial role in network construction, but is necessarily always arbitrary. At least two issues appear important for the network construction: (i) the connectivity measures should not occur by chance, and (ii) the networks changing in time should have the same connection density (similar number of links), providing a high sparsity level and economical network properties. In order to fulfill these two criteria, we first generated surrogate data through (i) creation of Gaussian white noise (cf.[1]) and (ii) a random permutation of the phase of the signals ("phase shuffling").

We first generated 224 20-s white noise signals, band-pass filtered them in the four frequency ranges (delta, theta, alpha, and beta), extracted the phase of the signals using the fast Hilbert transform, and then calculated the Phases Synchronization Index (*PSI*) using moving window approach between all possible channel pairs (24976) across 91 time windows. We first averaged these synchronization indices across the time widows and then calculated a mean (M) and standard deviation (SD) across the channel pairs, to determine the threshold as M + 2 SD. The same procedure was carried out with a real dataset, where the phases were shuffled and transformed back to the time domain using the inverse Fourier transform. In this way, we generate surrogate data with the same power spectrum as the real data but with a different time course. The M, SD, and thresholds determined as M + 2 SD for *PSI* in the four frequency bands with regard to the two types of surrogate data are presented in Table S1. It can be seen that *PSI* for phase-shuffled (PS) surrogate data was mostly higher than that for white noise (WN) surrogate data, and synchronization indices for real data (RD) are significantly higher than that for surrogate date (WN and PS). We then used the thresholds determined for PS surrogate data, as more conservative ones, and determined the costs of all

sets of RD that were analyzed in the study at the given threshold levels. The wiring costs (*K*) were calculated as the ratio of the number of actual connections ($N_{network}$) divided by the maximum possible number of connections in the network:

$$K = \frac{N_{network}}{N(N-1)} \cdot 100\%.$$

The result of this analysis is presented in Figure S2. It can be seen that the lowest cost level amounts to 20%. We therefore set the cost level for network analyses to this cost level that fulfills both our criteria, that is, the connectivity measures do not occur by chance and it corresponds to a high sparsity level providing economical network properties. This allowed a more accurate examination of the network topology in the different musical pieces and sequences.

Calculation of the graph-theoretical approach (GTA) measures

Network strengths. As *PSI* is a weighted symmetric measure, we obtained the node's strength (S_i^w) as the sum of weights of all connections (w_{ij}) to node *i*:

$$S_i^w = \sum_{j \in N} w_{ij} .$$

Strengths were determined for each node *i* separately for within-brain (*SwB*) and between-brain (*SbB*) connections. For the *common* hyperbrain network (HBN) analysis, *SbB* were determined in the whole HBN including all connections between the guitarist and audience participants with regard to the particular node *i*.

Clustering coefficient (*CC*) and characteristic path length (*CPL*). If the nearest neighbors of a node are also directly connected to each other, they form a cluster. For an individual node *i*, the CC_i^w is defined as the proportion of the number of pairs of *i*'s neighbors that are connected to the total number of pairs of *i*'s neighbors. In the case of a weighted undirected graph, the mean *CC* is calculated by the formula:[2]

$$CC = \frac{1}{N}\sum_{i \in N} CC_i^w = \frac{1}{N}\frac{2}{k_i(k_i - 1)}\sum_{j,h}\left(\hat{w}_{ij}\,\hat{w}_{ih}\,\hat{w}_{jh}\right)^{1/3},$$

where CC_i^w is the weighted *CC* of the node *i*, *N* is the number of nodes in the network, k_i is the degree of the node *i*, and the weights $\hat{w}_{ij}\,\hat{w}_{ih}\,\hat{w}_{jh}$ have been scaled relative to the maximum edge weight in the network, such that $\hat{w}_{ij} \leftarrow w_{ij} / \max(w)$. The *CC* measures the clustering or cliquishness of a typical neighborhood and is thus a measure of *network segregation*.

Another important measure is the *CPL*. In the case of an unweighted graph, the shortest path length or distance d_{ij} between two nodes *i* and *j* is the minimal number of edges that have to be passed to go from *i* to *j*. This is also called the geodesic path between the nodes *i* and *j*. For the weighted graph, the *CLP* is the weighted mean of the path lengths between all possible pairs of vertices:[3]

$$CPL = \frac{1}{N}\sum_{i \in N} L_i = \frac{1}{N(N-1)}\sum_{j \in N, j \neq i} d_{ij}^w,$$

where L_i is the average shortest path length from node *i* to all other nodes; the distance d_{ij}^w between two nodes *i* and *j* was calculated by remapping it to 1 – w_{ij} instead of the reciprocal of the edge weights ($1/w_{ij}$) to avoid the infinity problem if there is no path between any two nodes. *CPL* shows the degree of network integration, with a short *CPL* indicating higher *network integration*.

Global (E_{global}) and local (E_{local}) efficiency. Global efficiency *(E_{global})* is defined as the average inverse shortest path length and is calculated as follows:[4]

$$E_{global} = \frac{1}{N}\sum_{i \in N} E_{noda(i)}^w = \frac{1}{N(N-1)}\sum_{j \in N, j \neq i}\frac{1}{d_{ij}^w},$$

where $E_{noda(i)}^w$ is nodal efficiency of the node *i* determined as the normalized sum of the reciprocal of the shortest path length from a given node to all other nodes in the network.

Note that the distance d_{ij}^{w} between two nodes *i* and *j* in this case was calculated by remapping to the reciprocal of the edge weights ($1/w_{ij}$), because the reciprocal of the path length between disconnected nodes is zero (the inverse of infinity) and thus the harmonic mean is necessarily finite (cf.[5]). Like *CPL*, E_{global} is a measure of the integration of a network, but *CPL* is primarily influenced by long paths, whereas E_{global} is primarily influenced by short ones.

Local efficiency (E_{local}) is similar to the *CC* and is calculated as the harmonic mean of neighbor-neighbor distances:[4]

$$E_{local} = \frac{1}{N}\sum_{i\in N} E_{local(i)}^{w} = \frac{1}{N}\sum_{i\in N} \frac{\sum_{j,h\in G_i} (d_{jh}^{w})^{-1}}{N_{G_i}\left(N_{G_i}-1\right)},$$

where N_{G_i} is the number of nodes in subgraph G_i, comprising all nodes that are immediate neighbors of the node *i* (excluding the node *i* itself), and $E_{local(i)}^{w}$ is local efficiency of the node *i* determined as the reciprocal of the shortest path length between neighbors *j* and *h*. Thus, E_{local} of node *i* is defined with respect to the subgraph comprising all of *i*'s neighbors, after removal of node i and its incident edges.[4] Like *CC*, E_{local} is a measure of the segregation of a network, indicating efficiency of information transfer in the immediate neighborhood of each node and showing how fault-tolerant the system is.

All GTA measures described here were first determined for each of the nodes in the network and then averaged for specific brain regions and participant. Therefore, *N* in the formulas denotes the number of nodes in this specific sets or subunits in the network.

Modularity analysis and community structure determination

Modularity analysis was applied to detect optimized community structures or modules.[6,7] For this calculation, the modularity optimization method for weighted networks as implemented in the Brain Connectivity Toolbox (https://sites.google.com/site/bctnet/) was used.[8] The optimal community structure is a subdivision of the network or graph into non-overlapping groups of nodes in a way that maximizes the number of within-module edges, and minimizes

the number of between-module edges. The modularity (M^w) is a statistic that quantifies the degree to which the network may be subdivided into such clearly delineated groups or modules. For weighted networks, it is given by the formula:[6]

$$M^w = \frac{1}{l^w} \sum_{j \in N} \left[w_{ij} - \frac{k_i^w k_j^w}{l^w} \right] \cdot \delta_{m_i m_j},$$

where l^w is the total number of weights in the network, N is the total number of nodes in the network, w_{ij} are connection weights, k_i^w and k_j^w are weighted degrees or strengths of the nodes, m_i is the module containing node *i*, and δ_{m_i,m_j} is the Kronecker delta, where $\delta_{m_i,m_j} = 1$ if $m_i = m_j$, and 0 otherwise. High modularity values indicate the strong separation of the nodes into modules. $M^w = 0$ if nodes are randomly placed into modules or if all nodes belong to the same cluster, values around 0.3 or more usually indicate good divisions, and the maximum possible value of M^w is 1.[6]

To investigate the dynamic changes of modular structures across time, we used normalized mutual information (*MI*), which measures the similarity between two partitions and is given by the formula:[9]

$$MI(X,Y) = \frac{I(X,Y)}{\sqrt{H(X)H(Y)}},$$

where *I(X, Y)* denotes the mutual information between *X* and *Y*, and *H(X)* and *H(Y)* denote the entropy of *X* and *Y*, respectively.

Calculation of Granger Causality

To investigate the causal associations between guitar sounds and brain dynamics of the guitarists and audience, we used multivariate Granger Causality (*GC*) based on MultiVariate AutoRegressive (MVAR) modeling. *GC* in its original formulation is a bivariate concept but it could be extended to multivariate one (cf.[10]). Giving two time series x_1 and x_2, the model

considered by Granger[11] assumes that $x_1(t)$ and $x_2(t)$, with $t = 1, \ldots, T$, are represented by an univariate AR model of order p as:

$$x_1(t) = \sum_{k=1}^{p} a_1(k) x_1(t-k) + u_1(t)$$
$$x_2(t) = \sum_{k=1}^{p} a_2(k) x_2(t-k) + u_2(t)$$

where the prediction error for a time series depends only on its own past, and by a bivariate ARX model as:

$$x_1(t) = \sum_{k=1}^{p} a_{1.1}(k) x_1(t-k) + \sum_{k=1}^{p} a_{1.2}(k) x_2(t-k) + w_1(t)$$
$$x_2(t) = \sum_{k=1}^{p} a_{2.2}(k) x_2(t-k) + \sum_{k=1}^{p} a_{2.1}(k) x_1(t-k) + w_2(t)$$

where the prediction error depends on the past of the both signals. This model can also be extended to Q signals $x_1, x_2, \ldots, x_Q$:[10]

$$\begin{bmatrix} x_1(t) \\ \vdots \\ x_Q(t) \end{bmatrix} = \sum_{k=1}^{p} A_k \begin{bmatrix} x_1(t-k) \\ \vdots \\ x_Q(t-k) \end{bmatrix} + \begin{bmatrix} w_1(t) \\ \vdots \\ w_Q(t) \end{bmatrix}$$

with

$$A_k = \begin{bmatrix} a_{1.1}(k) & a_{1.2}(k) & \cdots & \cdots & a_{1.Q}(k) \\ \vdots & \vdots & \vdots & \vdots & \vdots \\ \vdots & \vdots & \vdots & a_{n.m}(k) & \vdots \\ \vdots & \vdots & \vdots & \vdots & \vdots \\ a_{Q.1}(k) & \cdots & \cdots & \cdots & a_{Q.Q}(k) \end{bmatrix}.$$

A_k is the matrix of autoregressive coefficients for the k^{th} time lag evaluating linear interaction of $x_m(t-k)$ on $x_n(t)$, while p is the model order that gives the maximum number of time lags.

In the case of the bivariate Granger Causality, the unbiased variance of prediction error $\Sigma_{x_2|x_2^-}$ for the univariate AR model is given by:

$$\Sigma_{x_2|x_2^-} = \frac{1}{T-p} \sum_{t=1}^{T} u_2^2(t) = \frac{RSS_{x_2|x_2^-}}{T-p}$$

and the unbiased variance of prediction error $\Sigma_{x_2|x_2^- x_1^-}$ for the bivariate ARX model could be determined as:

$$\Sigma_{x_2|x_2^- x_1^-} = \frac{1}{T-2p}\sum_{t=1}^{T} w_2^2(t) = \frac{RSS_{x_2|x_2^- x_1^-}}{T-2p}$$

where $RSS_{x_2|x_2^-}$ and $RSS_{x_2|x_2^- x_1^-}$ are the residual sums of squares in the corresponding models.

If X_1 causes X_2 in the Granger sense, then $\Sigma_{x_2|x_2^- x_1^-}$ must be smaller than $\Sigma_{x_2|x_2^-}$. The level of linear causality is then estimated by

$$GC_{x_2 \leftarrow x_1} = \ln \frac{\Sigma_{x_2|x_2^-}}{\Sigma_{x_2|x_2^- x_1^-}} .$$

In the multivariate case, the causality from x_m to x_n could be obtained in analog way as

$$GC_{x_n \leftarrow x_m} = \ln \frac{\Sigma_{x_n|x_1^- \ldots x_{m-1}^- x_{m+1}^- x_Q^-}}{\Sigma_{x_n|x_1^- \ldots x_Q^-}} = \ln \frac{(T-Qp)}{(T-(Q-1)p)} \frac{RSS_{x_n|x_1^- \ldots x_{m-1}^- x_{m+1}^- x_Q^-}}{RSS_{x_n|x_1^- \ldots x_Q^-}}$$

where $RSS_{x_n|x_1^- \ldots x_Q^-}$ is the residual sum of squares for a variable x_n in the model involving all variables, and $RSS_{x_n|x_1^- \ldots x_{m-1}^- x_{m+1}^- x_Q^-}$ is the one for the same model involving all variables except x_m.

Statistical evaluation of the multivariate *GC* was performed by the Fisher's test:[10]

$$F^{GC}_{x_n \leftarrow x_m} = \frac{(T-Qp)}{p} \frac{RSS_{x_n|x_1^- \ldots x_{m-1}^- x_{m+1}^- x_Q^-} - RSS_{x_n|x_1^- \ldots x_Q^-}}{RSS_{x_n|x_1^- \ldots x_Q^-}},$$

with $df_1 = p$ and $df_2 = (T - Qp)$.

References

1. Tass P., M.G. Rosenblum, J. Weule, *et al.* 1998. Detection of n:m Phase Locking from Noisy Data: Application to Magnetoencephalography. *Phys. Rev. Lett.* **81**: 3291–3294.
2. Onnela J.-P., J. Saramäki, J. Kertész, *et al.* 2005. Intensity and coherence of motifs in weighted complex networks. *Phys. Rev. E* **71**: 065103(R).
3. Watts D.J. & S.H. Strogatz. 1998. Collective dynamics of "small-world" networks. *Nature* **393**: 440–442.
4. Latora V. & M. Marchiori. 2001. Efficient Behavior of Small-World Networks. *Phys. Rev. Lett.* **87**: 198701.
5. Fornito A., A. Zalesky & E. Bullmore. 2016. "*Fundamentals of Brain Network Analysis*." London: Elsevier Inc.
6. Newman M.E.J. 2004. Analysis of weighted networks. *Phys. Rev. E* **70**: 1–9.
7. Newman M.E.J. 2006. Finding community structure in networks using the eigenvectors of matrices. *Phys. Rev. E* **74**: 036104.
8. Rubinov M. & O. Sporns. 2010. Complex network measures of brain connectivity: uses and interpretations. *Neuroimage* **52**: 1059–69.
9. Strehl A. & J. Ghosh. 2003. Cluster ensembles - A knowledge reuse framework for combining multiple partitions. *J. Mach. Learn. Res.* **3**: 583–617.
10. Gourévitch B., R. Le Bouquin-Jeannès & G. Faucon. 2006. Linear and nonlinear causality between signals: Methods, examples and neurophysiological applications. *Biol. Cybern.* **95**: 349–369.
11. Granger C.W.J. 1969. Investigating Causal Relations by Econometric Models and Cross-spectral Methods. *Econometrica* **37**: 424–438.

Supplementary Table and Supplementary Figures

Table S1

Mean (M) and standard deviation (SD) of Phase Synchronization Index (*PSI*) values for white noise (WN) and phase-shuffled (PS) surrogate data, and for real data (RD) in the four frequency bands

	WN			PS			RD		t-value
	M	SD	M+2SD	M	SD	M+2SD	M	SD	RD>PS
delta	0.265	0.035	0.335	0.305	0.043	0.391	0.347	0.118	54.4***
theta	0.249	0.033	0.315	0.249	0.034	0.317	0.288	0.129	46.9***
alpha	0.204	0.028	0.260	0.210	0.030	0.270	0.240	0.131	37.0***
beta	0.126	0.017	0.160	0.130	0.018	0.166	0.177	0.150	49.7***

WN, White Noise; PS, phase-shuffled; RD, real data; *PSI*, Phase Synchronization Index; M + 2SD indicates network threshold for the two types of surrogate data; t-values were calculated between RD and PS surrogate data; ***, $P < 0.0001$.

Figure S1. Scene of the concert with a quartet of guitarists and audience.

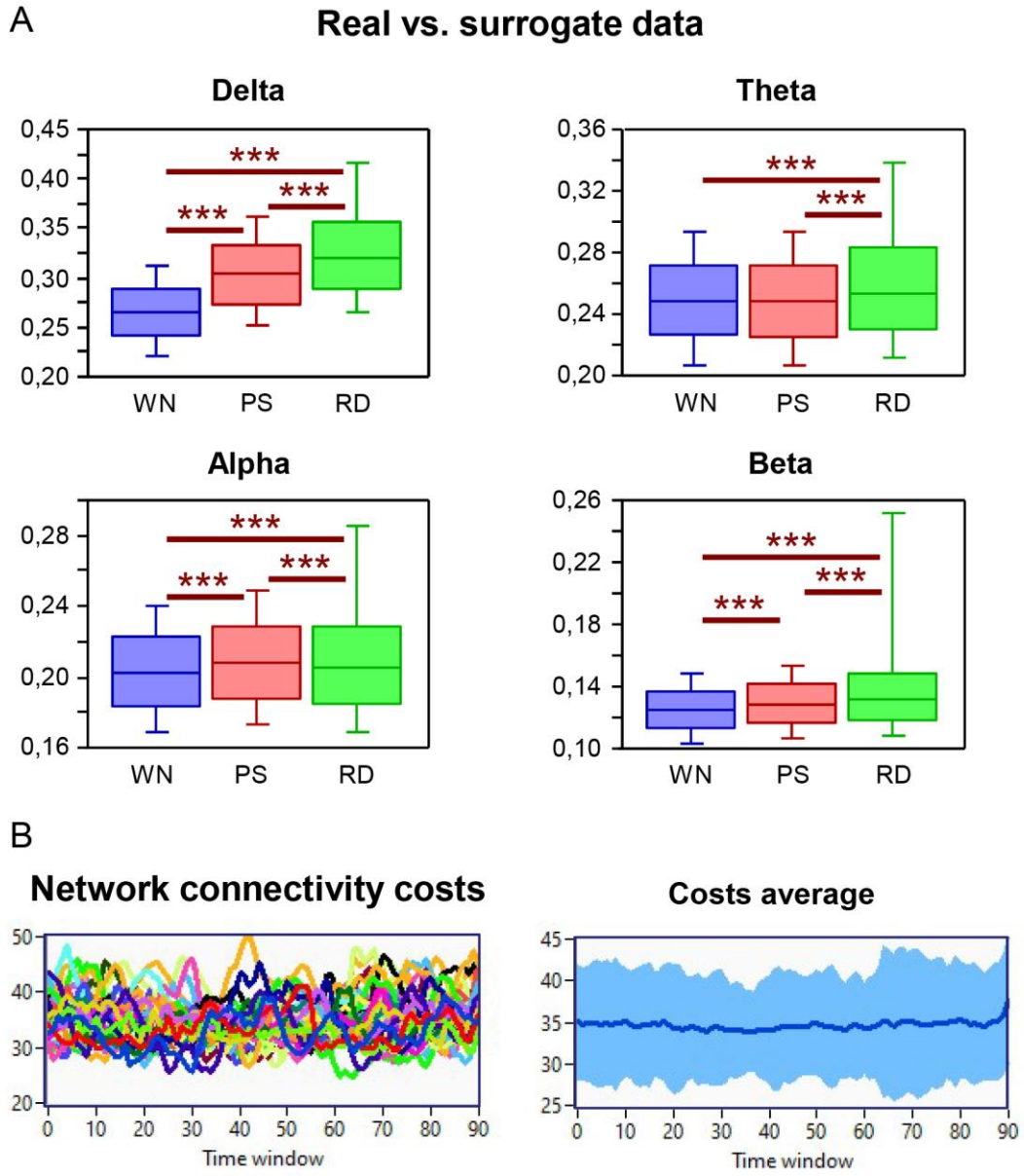

Figure S2. Real and surrogate data and network connectivity costs. (A) Box plots for real and surrogate data across the four frequency bands. For this representation, the Phase Synchronization Index (PSI) values were first averaged across the time windows for each of the network connections. (B) Network connectivity or wiring costs across the different time windows. For this representation, the hyperbrain networks (HBNs) of all real data investigated in the study were constructed by using the threshold determined as the mean + two standard deviations (SDs) of phase-shuffled surrogate data and then HBN costs were calculated for all the data at the four frequency bands across the 91 time windows. The results of these calculations are presented on the left. On the right, the average costs + two SDs are displayed. They are all higher than 20%. WN, white noise surrogate data; PS, phase-shuffled surrogate data; RD, real data; ***, $P < 0.001$.

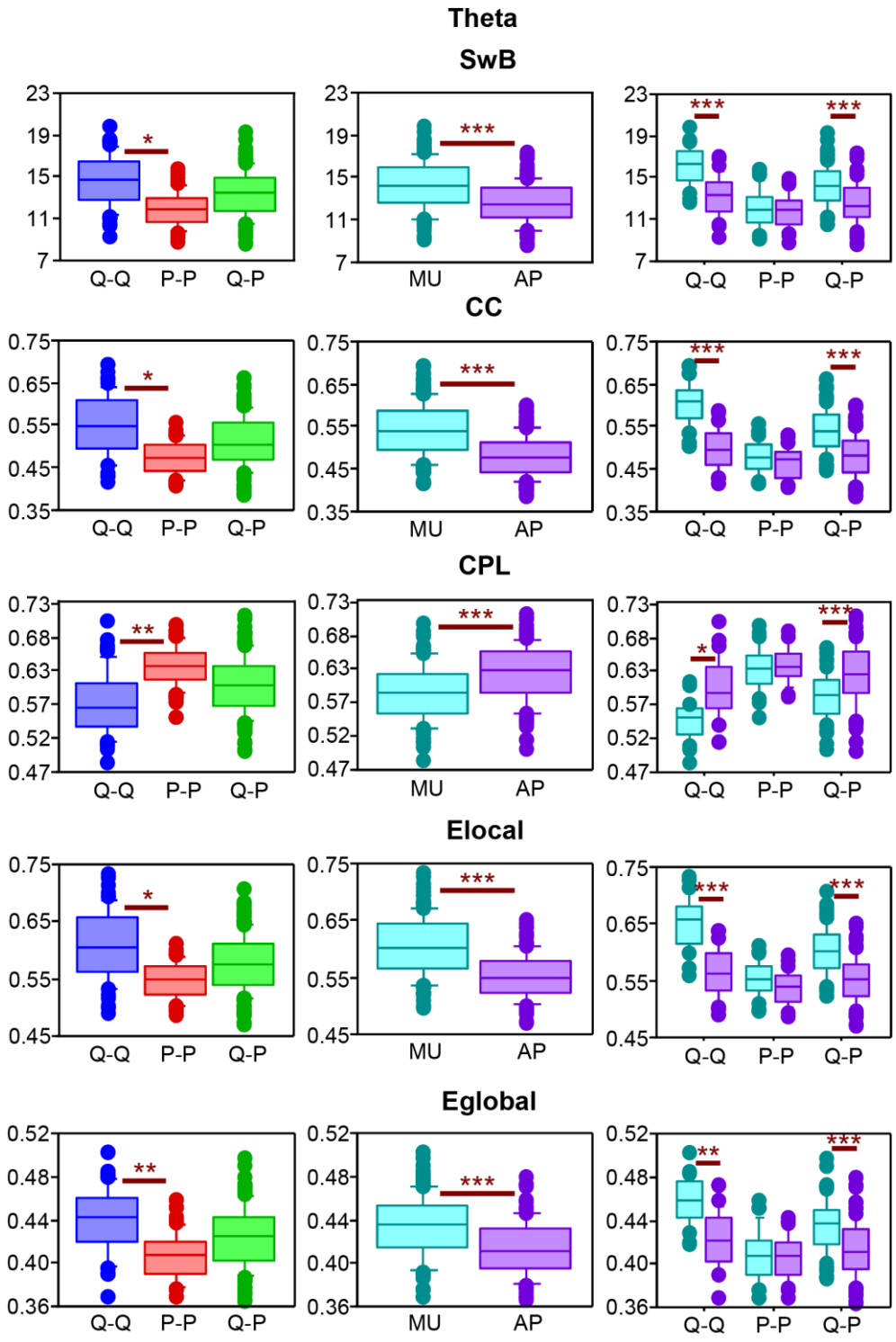

Figure S3. ANOVA results for the *dual* HBN indices in the theta frequency band. Main effects of the factors Group (Q-Q, Q-P, and P-P) and Condition (MU vs. AP) and their interaction are presented as box plots. *SwB*, strength within brains; *CC*, clustering coefficient; *CPL*, characteristic path length; E_{local}, local efficiency; E_{global}, global efficiency; Q-Q, quartet-quartet dual networks; Q-P, quartet-public dual networks; P-P, public-public dual networks; MU, music condition; AP, applause; *, $P < 0.05$; **, $P < 0.01$; ***, $P < 0.001$.

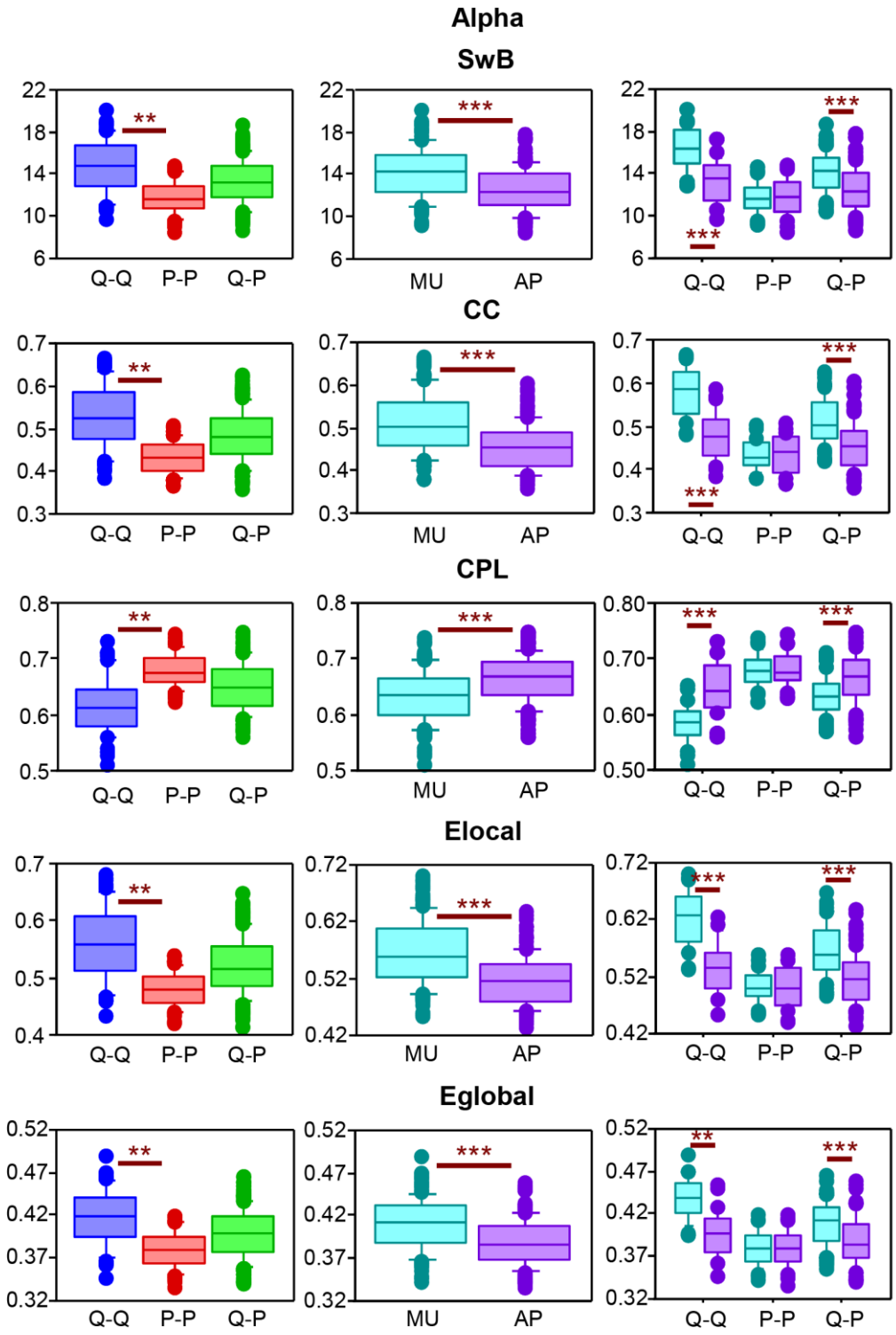

Figure S4. ANOVA results for the *dual* HBN indices in the alpha frequency band. Main effects of the factors Group (Q-Q, Q-P, and P-P) and Condition (MU vs. AP) and their interaction are presented as box plots. *SwB*, strength within brains; *CC*, clustering coefficient; *CPL*, characteristic path length; E_{local}, local efficiency; E_{global}, global efficiency; Q-Q, quartet-quartet dual networks; Q-P, quartet-public dual networks; P-P, public-public dual networks; MU, music condition; AP, applause; *, $P < 0.05$; **, $P < 0.01$; ***, $P < 0.001$.

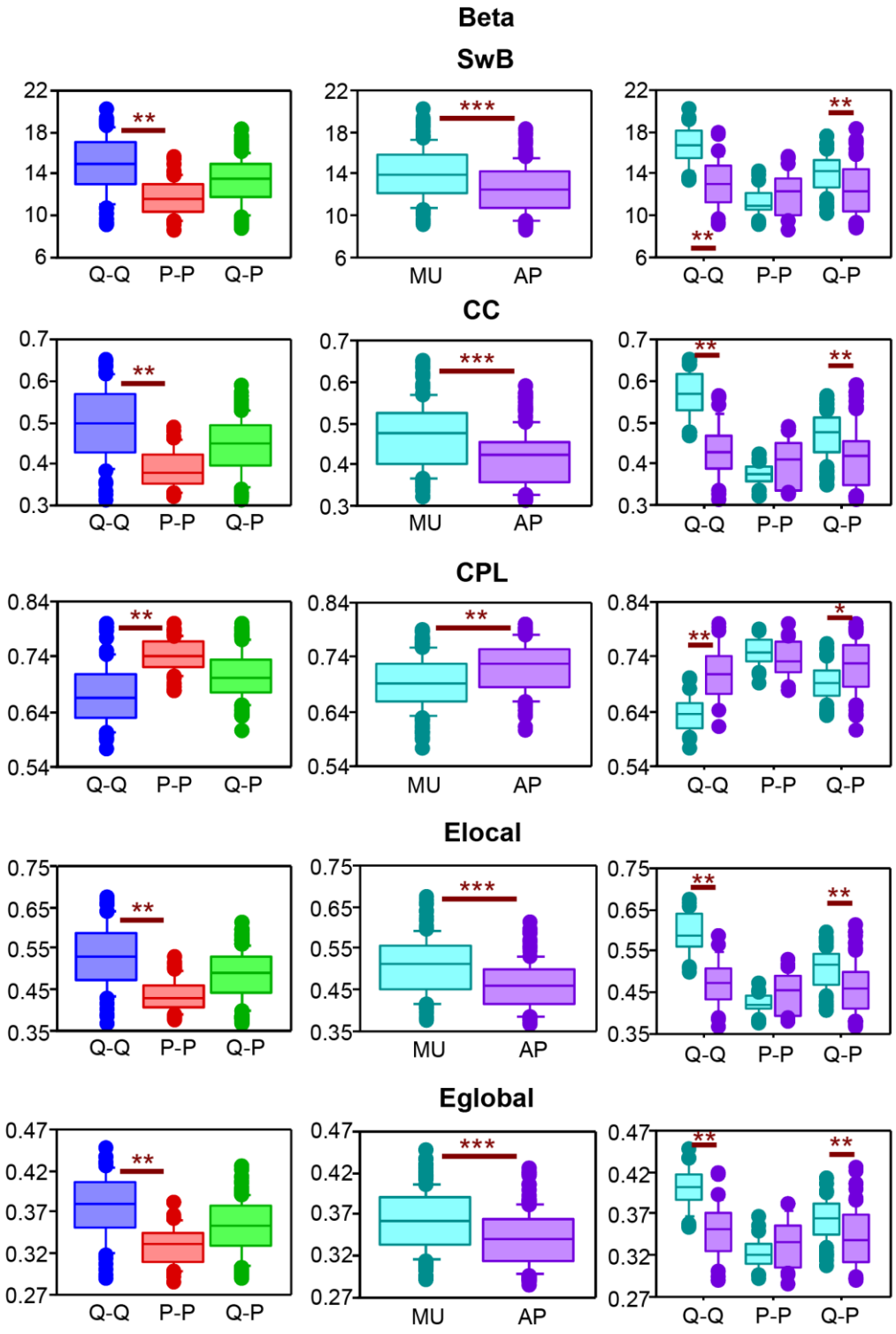

Figure S5. ANOVA results for the *dual* HBN indices in the beta frequency band. Main effects of the factors Group (Q-Q, Q-P, and P-P) and Condition (MU vs. AP) and their interaction are presented in a form of the box plots. *SwB*, strength within brains; *CC*, clustering coefficient; *CPL*, characteristic path length; E_{local}, local efficiency; E_{global}, global efficiency; Q-Q, quartet-quartet dual networks; Q-P, quartet-public dual networks; P-P, public-public dual networks; MU, music condition; AP, applause; *, $P < 0.05$; **, $P < 0.01$; ***, $P < 0.001$.

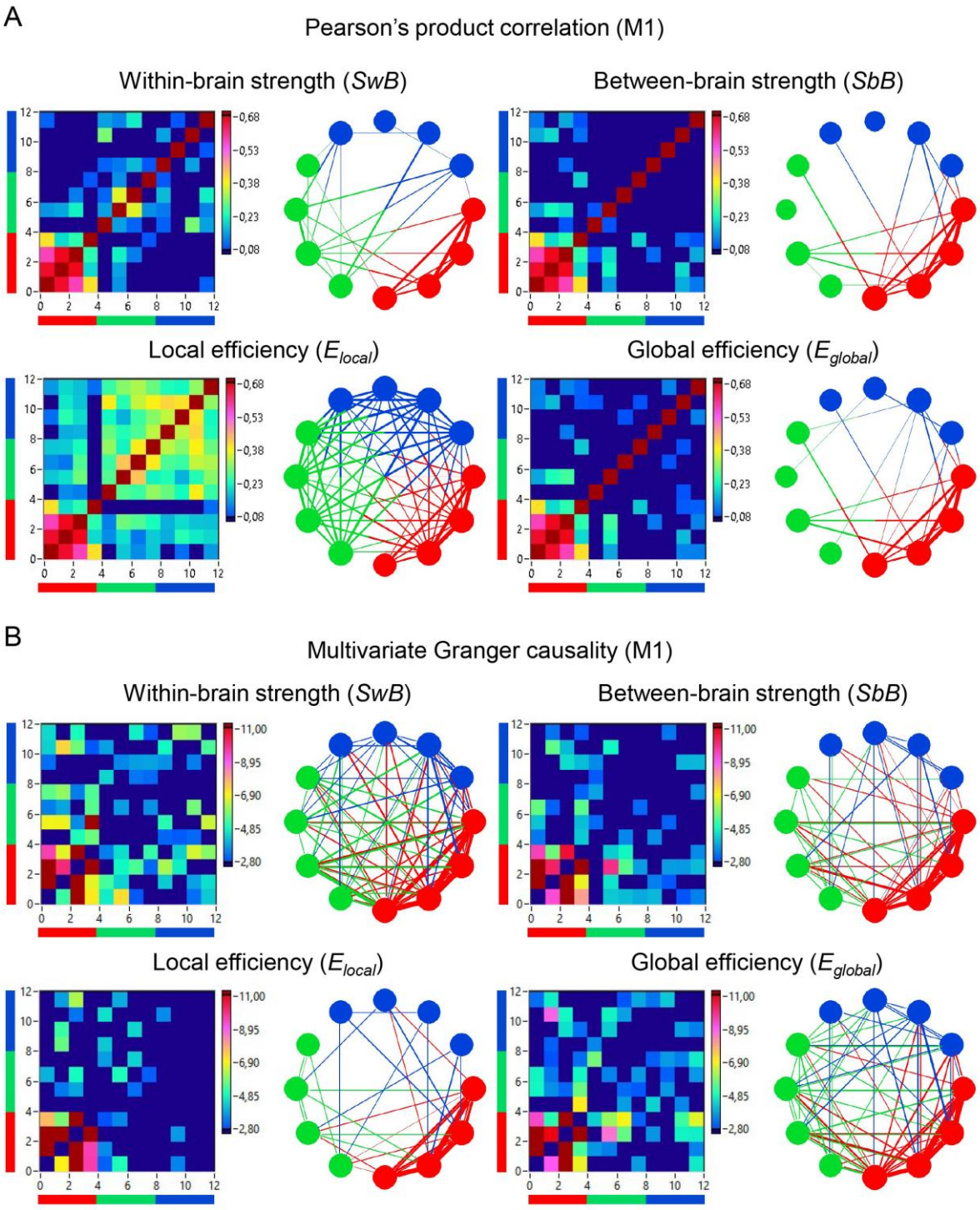

Figure S6. Linear and causal relationships between MSD and NTD indices for the music piece 1. (A) Linear relationships indicated by Pearson's product correlation. (B) Causal relationships indicated by multivariate Granger causality. The relationships are presented in form of matrices or heatmaps and circular connectivity maps. In the connectivity maps, the four red circles or nodes represent the four guitar sounds, the four green circles represent the four guitarists' brains, and the four blue circles represent the four audience members' brains. The linear relationships are symmetric and the causal relationships are asymmetric. The direction of the links is coded by color. Note that the links in causal connectivity maps are either unidirectional or bidirectional.

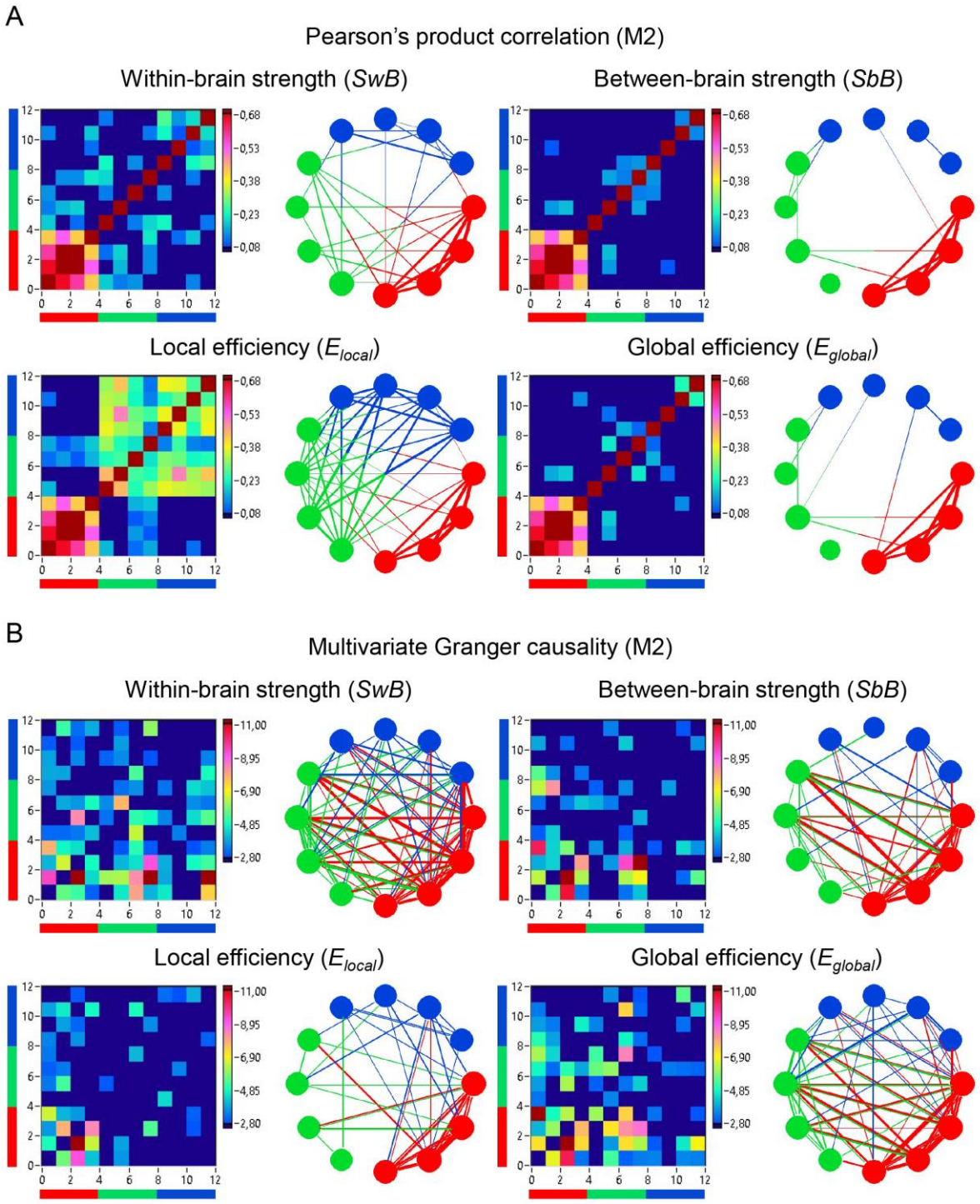

Figure S7. Linear and causal relationships between MSD and NTD indices for the music piece 2. (A) Linear relationships indicated by Pearson's product correlation. (B) Causal relationships indicated by multivariate Granger causality. The relationships are presented in form of matrices or heatmaps and circular connectivity maps. In the connectivity maps, the four red circles or nodes represent the four guitar sounds, the four green circles represent the four guitarists' brains, and the four blue circles represent the four audience members' brains. The linear relationships are symmetric and the causal relationships are asymmetric. The direction of the links is coded by color. Note that the links in causal connectivity maps are either unidirectional or bidirectional.

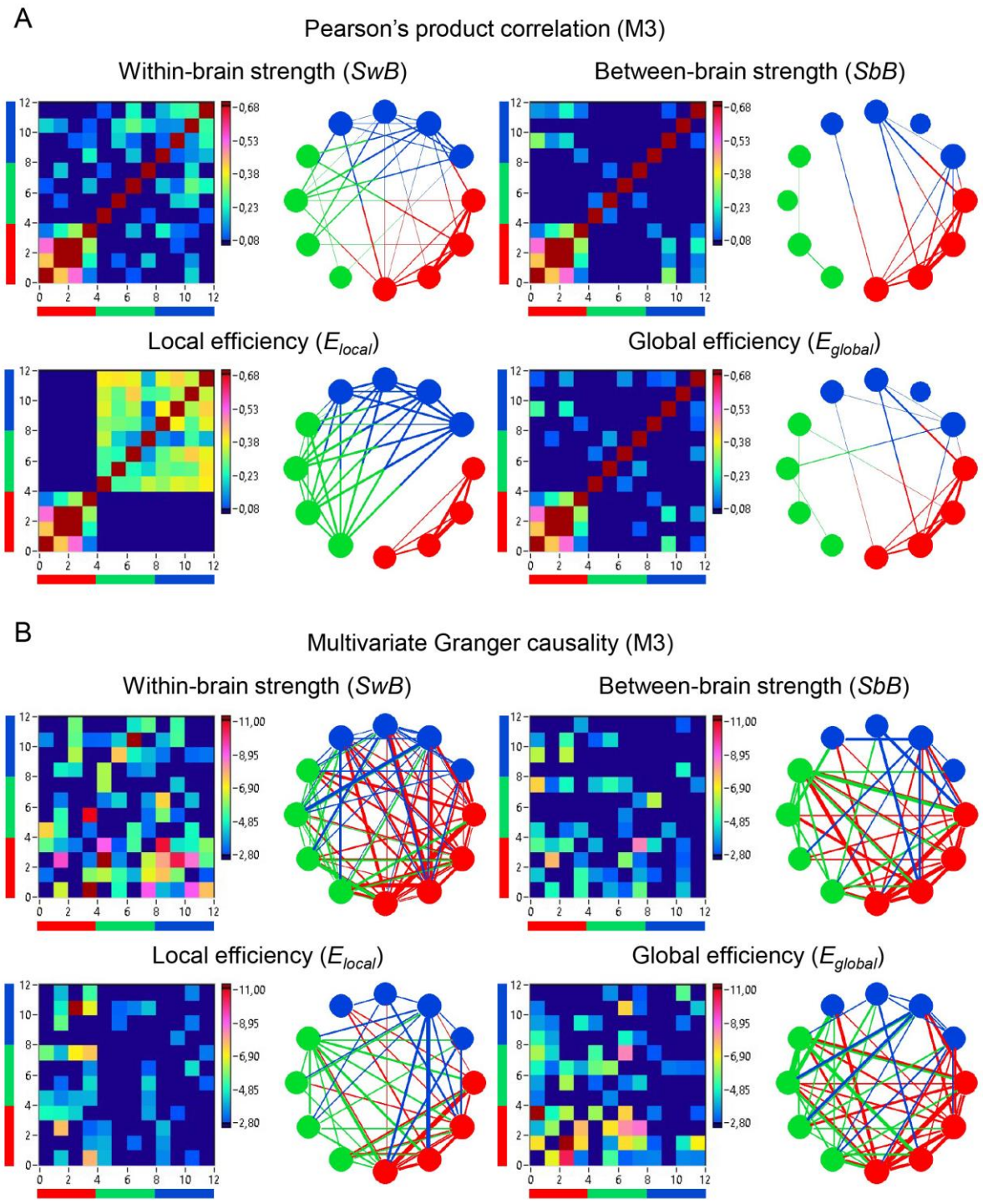

Figure S8. Linear and causal relationships between MSD and NTD indices for the music piece 3. (A) Linear relationships indicated by Pearson's product correlation. (B) Causal relationships indicated by multivariate Granger causality. The relationships are presented in form of matrices or heatmaps and circular connectivity maps. In the connectivity maps, the four red circles or nodes represent the four guitar sounds, the four green circles represent the four guitarists' brains, and the four blue circles represent the four audience members' brains. The linear relationships are symmetric and the causal relationships are asymmetric. The direction of the links is coded by color. Note that the links in causal connectivity maps are either unidirectional or bidirectional.